Article

Journal of Vibration and Control
2018, Vol. 24(16) 3684–3697

DOI: 10.1177/1077546317709387
journals.sagepub.com/home/jvc
SAGE

Using passive control by a pendulum in a portal frame platform with piezoelectric energy harvesting

Rodrigo T Rocha[1], Jose M Balthazar[2,3], Angelo M Tusset[1] and Vinicius Piccirillo[1]

Abstract

This work presents a passive control strategy using a pendulum on a simple portal frame structure, with two-to-one internal resonance, with a piezoelectric material coupling as a means of energy harvesting. In addition, the system is externally base-excited by an electro-dynamical shaker with harmonic output. Due to internal resonance the system may present the phenomenon of saturation, which provides some nonlinear dynamical behavior to the system. A pendulum is coupled to control nonlinear behaviors, leading to a periodic orbit, which is necessary to maintain energy harvesting. The results show that the system presents, most of the time, as being quasiperiodic. However, it does not present as being chaotic. With the pendulum, it was possible to control most of these quasiperiodic behaviors, leading to a periodic orbit. Moreover, it is possible to eliminate the need for an active or semi-active control, which are usually more complex. In addition, the control provides a way to detune the energy captured to the desired operating frequency.

Keywords

Passive control, saturation phenomenon, energy harvesting, internal resonance, electro-dynamical shaker

1. Introduction

In recent decades, research into electro-mechanical systems that are able to scavenge/harvest energy from an operating environment has increased substantially. Vibration-based energy harvesting is the most studied form in recent years, and these systems are usually excited by wind, sea waves and vehicle traffic, i.e. external excitation. In addition, with technological advances, smaller devices with low power consumption have been developed. Most use a battery as an energy source. However, batteries are finite energy sources, which require recharging or replacement. Thus, one of the most promising and studied devices as a means of low power energy harvesting are piezoelectric materials, which convert mechanical energy into electrical energy.

Piezoelectric materials have shown themselves to be a great means of low power transduction, and have been widely studied by Preumont (2006), Stephen (2006), DuToit and Wardle (2007), Twiefel et al. (2008), Erturk et al. (2009), Jalili (2009), Priya and Inman (2009), Stanton et al. (2010), Erturk and Inman (2011), Litak et al. (2012), Friswell et al. (2015), Litak et al. (2015) and Syta et al. (2015), among others. These authors studied the materials in different devices, for example, as a piezomagnetoelastic structure and device harvesting energy from environmental vibration, exploring the reuse of wasted vibration energy in the environment, which is a very important subject because of the search for new, mainly renewable, energy sources.

However, these materials present certain nonlinearities related to their strain constants. There is a nonlinear relation between the strain and the electric field of a piezoelectric material (DuToit and Wardle, 2007; Twiefel et al., 2008). Crawley and Anderson (1990) identified experimentally these nonlinearities showing

[1]Federal University of Technology, Brazil
[2]Aeronautics Technological Institute, Brazil
[3]Sao Paulo State University, Brazil

Received: 9 May 2016; accepted: 18 April 2017

Corresponding author:
Rodrigo T Rocha, Federal University of Technology, Department of Electronics, Av. Monteiro Lobato, Neighborhood: Jardim Carvalho, 83016-210, Ponta Grossa – PR, Parana, Brazil.
Email: digao.rocha@gmail.com

their relevance to the nonlinear theoretical model and the experimental model. Because of this, an analytical approximation of the nonlinearities of the material was proposed by Triplett and Quinn (2009). A recent and complete review of these properties was presented by Daqaq et al. (2014). As the nonlinearities became an important feature for the usage of these materials, many authors introduced the nonlinear piezoelectric coupling to their work and showed that energy harvesting can be more or less efficient. In particular we mention the works of Iliuk et al. (2013a, 2013b), Balthazar et al. (2014) and Iliuk et al. (2014).

The piezoelectric material, generally, is coupled to a main structure that will vibrate, causing deformation of the ceramic, consequently transforming the vibration energy into electrical energy. However, a structure with two degrees of freedom contains some nonlinearities because of the coupling. In particular, some can be coupled with an associated quadratic nonlinearity under a two-to-one internal resonance. Because of these conditions, when these systems are subjected to a resonant external excitation, one of the degrees of freedom transfers part of its available vibratory energy to the other one. This is a phenomenon called saturation, as described by many authors, for example Nayfeh et al. (1973), Mook et al. (1985), Nayfeh (2000), Mankala and Quinn (2004), Quinn (2007) and Nayfeh and Mook (2008). The implementation of saturation as a control method was proposed by Golnaraghi (1991), Oueini et al. (1997), Oueini (1999) and Pai and Schulz (2000), and studied by Pai et al. (1998), Felix at al. (2005), Shoeybi and Ghorashi (2005), Warminski et al. (2013), Felix et al. (2014) and Tusset et al. (2015), among others.

However, the saturation phenomenon may present some nonperiodic motions because of its high level of instability (Nayfeh and Mook, 2008). Besides, energy harvesting needs stable periodic behavior to maintain harvesting. Therefore, the implementation of a passive control strategy is considered.

The study of a passive controller is shown to be very useful for the control of some nonperiodic motions that tend to a periodic orbit. In particular, the work of Iliuk et al. (2013a) considered a model of energy harvester based on a simple portal frame with a single-degree-of-freedom structure. The system was considered as a nonideal system (NIS) due to the full interaction of the structure's motion with the energy source, a DC motor with a limited power supply. Moreover, it was found to be a bi-stable Duffing oscillator presenting chaotic behavior. The nonlinear piezoelectric material was considered in the coupling mathematical model. The structure was controlled using a pendulum as a passive control and improved the energy harvesting of the system. In addition to that work, Iliuk et al. (2013b) considered a nonenergy sink (NES) passive control for the same model, which also very well controlled the chaotic behavior, which led to a periodic orbit. Advanced studies of passive controllers can be found in the works of Jiang et al. (2003), Musienk et al. (2006), Gourdon et al. (2007), Malatkar and Nayfeh (2007), Manevitch et al. (2007), Vakakis (2008), Luongo and Zulli (2012, 2013), Zulli and Luongo (2015) and Rocha et al. (2016), amongst others.

Therefore, as saturation phenomenon may present different kinds of behavior such as periodic, quasiperiodic and even chaotic behavior, this work will implement a passive control by a pendulum in order to investigate the best configuration for harvesting energy with periodic behavior.

The results showed that the passive controller is a good way to eliminate the need for an active or semi-active controller that need electricity for interaction. Thus, the energy harvesting is totally natural. Rocha et al. (2015) studied the influence of a pendulum in a simple portal frame of two degrees of freedom with harmonic base excitation. The system presented chaotic behavior and, with the usage of a pendulum, control and tuning of the energy harvesting of the system was possible.

However, in this work, the external excitation is simulated by an electro-dynamical shaker, of which the mechanical and electrical parts are considered (Wang and Jing, 2004; Xu et al., 2005, 2007; Lenci et al., 2008; Litak et al., 2010; Lenci and Rega, 2011; Yokoi and Hikihara, 2011; Lenci et al., 2012; Alevras et al., 2014; Avanço et al., 2015). The main reason for using this shaker is that we can simulate theoretically the influence of the shaker and, in the future, prove experimentally the results. This work, however, is entirely theoretical.

This work is organized as follows. In the first section we introduce the motivation for this work. Section 2 shows the modeling of the full system through the energy method of Lagrange. The next section presents the parameters and some numerical simulations of the system without the control. In the following section, the pendulum is considered as a passive controller and some numerical simulations are carried out to evaluate the usage of the control. Finally, the last section presents the conclusions from the work.

2. Modeling of portal frame platform energy harvesting

The energy harvesting model in this work, illustrated in Figure 1, consists of a structure with two degrees of freedom with piezoceramic material coupled to a column, a linear pendulum coupled to the mid-span of the beam, which is the passive controller of this

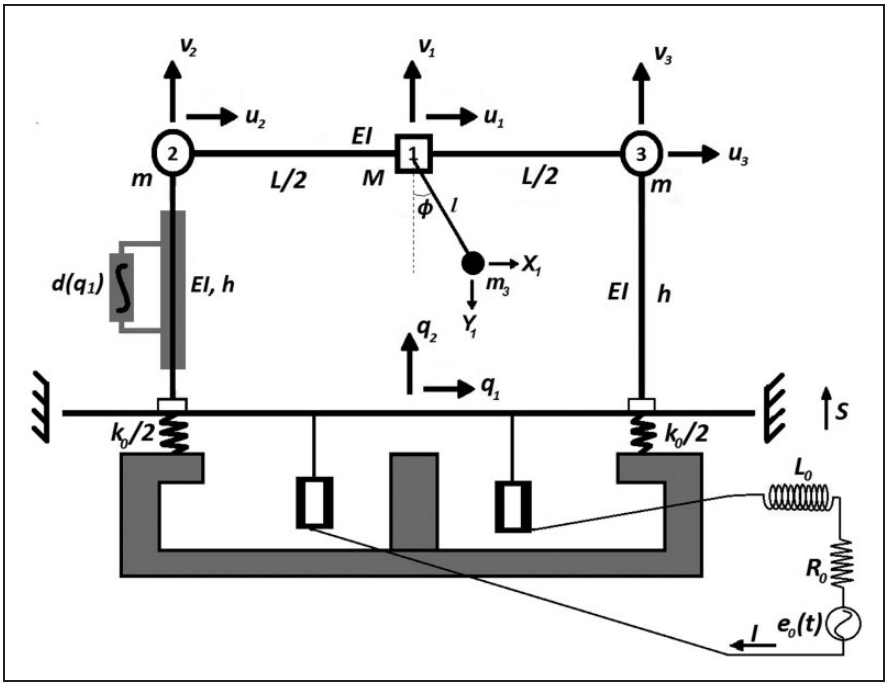

Figure 1. Portal frame platform physical model.

work, and an electro-dynamical shaker to base-excite the portal frame.

The portal frame consists of two columns clamped at their bases with height h and a horizontal beam pinned to the columns at both ends with length L. Both columns and beam have flexural stiffness EI. The mass at mid-span of the beam is M. We consider that m represents the masses of the columns. The structure is modeled as a lumped mass system with two degrees of freedom. The coordinate q_1 is related to the horizontal displacement (sway mode), with natural frequency ω_1, and q_2 is related to the vertical displacement (first symmetrical mode), with natural frequency ω_2. The generalized coordinates q_i are the displacements of the mass at the mid-span of the beam M. The linear stiffness of the columns and the beam can be evaluated by a Rayleigh–Ritz procedure using cubic trial functions. Geometric nonlinearity is introduced by considering the shortening due to bending of the columns and of the beam.

The linear pendulum is coupled to the mass of the mid-span of the beam, consisting of a mass m_3, rotational stiffness k_3 and rotational damping as c_3, with natural frequency ω_3.

The nonlinear piezoelectric material is distributed along the column as an electric circuit, which is excited by an internal voltage (back-emf) proportional to a mechanical velocity related to its deformation due to the vibration of the column where the electrical energy will be harvested. This circuit consists of a resistor R_p, a produced charge Q_p and a capacitance C_p of the capacitor. The dimensionless relation of nonlinearity of the piezoceramic is given by $\mathrm{d}(q_1) = \theta(1 + \Theta|q_1|)$ defined by Triplett and Quinn (2009), where θ is the linear piezoelectric coefficient and Θ is the nonlinear piezoelectric coefficient.

The mechanical system is base-excited by an electro-dynamical shaker whose output force is harmonic. The mechanical part of the shaker consists of a base with mass m_0, with displacement S, stiffness k_0 and damping c_0, with natural frequency ω_0. The electrical part is considered as a RL circuit, which possesses an inductance L_0, resistance R_0 and an output harmonic source with amplitude e_0 and frequency ω_n.

The frequency of the shaker is set to near resonance with the symmetric mode. Natural frequency of the symmetric mode ω_2 is also set to twice the natural frequency of the sway mode as $2\omega_1 = \omega_2$. These conditions of resonance are necessary to have modal coupling in the nonlinear adopted model, i.e. the saturation phenomenon occurs.

The natural frequencies of the structure are dependent on each other because they are coupled, i.e. they are evaluated with the presence of the pendulum and the excited base.

The modeling of the governing equations of the motion of the system is carried out below.

2.1. Modeling of the dynamical system

The modeling of the physical system was developed with Lagrange's energy method, which uses the Lagrangian function and the Euler–Lagrange equation.

Nodal displacements shown in Figure 1 are

$$\begin{aligned} &u_1 = q_1 \quad u_2 = u_1 + \frac{B}{4}v_1^2 \quad u_3 = u_1 - \frac{B}{4}v_1^2 \\ &v_1 = q_2 + S \quad v_2 = S - \frac{A}{2}u_1^2 \quad v_3 = S - \frac{A}{2}u_1^2 \\ &X_1 = u_1 + l\sin\phi \\ &Y_1 = v_1 - l\cos\phi \end{aligned} \tag{1}$$

where $A = 6/5h$ and $B = 24/5L$. The stiffness of the beam and column calculated by the Rayleigh–Ritz method are $k_b = 48EI/L^3$ and $k_c = 3EI/h^3$, respectively.

Using nodal displacements of equation (1), the kinetic energy is obtained, denoted by equation (2)

$$\begin{aligned} T = {} & \frac{1}{2}M\left(\dot{q}_1^2 + \dot{q}_2^2 + 2\dot{q}_2\dot{S} + \dot{S}^2\right) + \frac{1}{2}m\left(2\dot{q}_1^2 + 2\dot{S}^2 - 4Aq_1\dot{q}_1\dot{S}\right) \\ & + \frac{1}{2}m_0\dot{S}^2 + \frac{1}{2}L_0\dot{Q}_0^2 + \frac{1}{2}m_3\Big(\dot{q}_1^2 + \dot{q}_2^2 + 2\dot{q}_2\dot{S} + \dot{S}^2 \\ & + l^2\dot{\phi}^2 + 2l\dot{\phi}\Big(\dot{q}_1\cos\phi + \left(\dot{q}_2 + \dot{S}\right)\sin\phi\Big)\Big) \end{aligned} \tag{2}$$

The potential energy of the system is given by the strain energy of the structure, the stiffness of the pendulum, the work of the weight of the masses of the beam, columns and pendulum, and the stiffness of the shaker base. In addition is considered the electrical part of the piezoelectric circuit, with the contribution of the piezoelectric and the capacitor, and the electrical part of the shaker with its coupling through its base displacement with the electrical current of the shaker, i.e. the electromagnetic force of the device. The potential energy is given by equation (3)

$$\begin{aligned} V = {} & (k_c - mgA)q_1^2 + \frac{1}{2}k_b\left(q_2^2 + Aq_2q_1^2\right) + (M + 2m)gS \\ & + Mgq_2 + \frac{1}{2}k_0S^2 + K\dot{Q}_0S + m_3g(q_2 + S - l\cos\phi) \\ & + \frac{1}{2}k_3\phi^2 - \frac{\mathrm{d}(q_1)}{C_p}Q_p\left(q_1 + S + \frac{B}{4}q_2^2\right) + \frac{1}{2}\frac{Q_p^2}{C_p} \end{aligned} \tag{3}$$

The energy of dissipation of the system is considered, comprising the structure, pendulum and shaker damping defined by the Rayleigh function and the resistor of the electrical circuit. Then, in equation (4)

$$D = \frac{1}{2}c_1\dot{q}_1^2 + \frac{1}{2}c_2\dot{q}_1^2 + \frac{1}{2}c_0\dot{S}^2 + \frac{1}{2}c_3\dot{\phi}^2 + \frac{1}{2}R_0\dot{Q}_0^2 + \frac{1}{2}R_p\dot{Q}_p^2 \tag{4}$$

The unique external force is given by the electrical source of the shaker, which has a harmonic as in equation (5)

$$Q_{0_{ext}} = e_0\cos\omega_n t \tag{5}$$

Therefore, the Lagrangian function is defined by equation (6) and, using Euler–Lagrange, equation (7), we have the equations of motion of the system that are equations (8) to (11), (13) and (14)

$$L(\dot{q}_i, q_i, t) = T - V \tag{6}$$

$$\frac{d}{dt}\left(\frac{\partial L}{\partial \dot{q}_i}\right) - \frac{\partial L}{\partial q_i} + \frac{\partial D}{\partial \dot{q}_i} = F_{\text{ext}} \quad i = q_1, q_2, S, \phi, Q_0, Q_p \tag{7}$$

$$\begin{aligned} & (2m + M + m_3)\ddot{q}_1 + c_1\dot{q}_1 + 2(k_c - mgA)q_1 \\ & = -m_3l\left(\dot{\phi}^2\sin\phi - \ddot{\phi}\cos\phi\right) \\ & \quad + 2mA\dot{q}_1\dot{S} - k_bAq_1q_2 + \frac{\mathrm{d}(q_1)}{C_p}Q_p \end{aligned} \tag{8}$$

$$\begin{aligned} & (M + m_3)\left(\ddot{q}_2 + \ddot{S}\right) + c_2\dot{q}_2 + k_bq_2 + (M + m_3)g \\ & = -\frac{Ak_b}{2}q_1^2 - m_3l\left(\ddot{\phi}\sin\phi + \dot{\phi}^2\cos\phi\right) + \frac{\mathrm{d}(q_1)}{C_p}\frac{B}{2}Q_pq_2 \end{aligned} \tag{9}$$

$$\begin{aligned} & (M + 2m + m_0 + m_3)\ddot{S} + (M + m_3)\ddot{q}_2 \\ & \quad + (M + 2m + m_3)g + c_0\dot{S} + k_0S + K\dot{Q}_0 \\ & = 2mA\dot{q}_1^2 + m_3l\left(\ddot{\phi}\sin\phi + \dot{\phi}^2\cos\phi\right) + \frac{\mathrm{d}(q_1)}{C_p}Q_p \end{aligned} \tag{10}$$

$$\begin{aligned} & m_3l^2\ddot{\phi} + m_3l\left[\ddot{q}_1\cos\phi + \left(\ddot{q}_2 + \ddot{S}\right)\sin\phi\right] \\ & \quad + k_3\phi + c_3\dot{\phi} = m_3gl\sin\phi \end{aligned} \tag{11}$$

$$L_0\ddot{Q}_0 - K\dot{S} + R\dot{Q}_0 = e_0\cos\omega_n t \tag{12}$$

or, considering $I = \dot{Q}_0$, the equation for the electrical part of the shaker becomes equation (13)

$$L_0\dot{I} - K\dot{S} + RI = e_0\cos\omega_n t \tag{13}$$

$$R_p\dot{Q}_p - \tfrac{\mathrm{d}(q_1)}{C_p}\left(q_1 + S + \tfrac{B}{4}q_2^2\right) + \tfrac{Q_p}{C_p} = 0 \tag{14}$$

For a better analysis, a dimensionless process was carried out resulting in the dimensionless governing equations of motion of the system

$$\begin{aligned} x_1'' + \mu_1x_1' + x_1 = {} & \gamma_1\left(\phi'^2\sin\phi - \phi''\cos\phi\right) + \beta_1x_1'Y' \\ & - \alpha_1x_1x_2 + \theta(1 + \Theta|x_1|)\delta_1V \end{aligned} \tag{15}$$

$$x_2'' + \varepsilon Y'' + \mu_2 x_2' + \omega_2^2 x_2 + G_2 = -\alpha_2 x_1^2 - \gamma_2(\phi'' \sin\phi + \phi'^2 \cos\phi) + \theta(1 + \Theta|x_1|)\delta_2 x_2 V \quad (16)$$

$$Y'' + \delta_m x_2'' + \mu_0 Y' + \omega_0^2 Y + G_0 + \beta_3 U = \beta_4 x_1'^2 + - \gamma_0(\phi'' \sin\phi + \phi'^2 \cos\phi) + \theta(1 + \Theta|x_1|)\delta_1 V \quad (17)$$

$$\phi'' + \mu_3\phi' + \omega_3^2\phi + \gamma_3 x_1'' \cos\phi + (\gamma_4 x_2'' + \gamma_3 Y'')\sin\phi = \gamma_5 \sin\phi \quad (18)$$

$$U' - \beta_5 Y' + \rho U = E_0 \cos\Omega\tau \quad (19)$$

$$V' - \theta(1 + \Theta|x_1|)\left[\delta_3(x_1 + Y) + \delta_4 x_2^2\right] + \delta_3 V = 0 \quad (20)$$

where the dimensionless parameters are

$$x_1 = \frac{q_1}{h} \quad x_2 = \frac{q_2}{L} \quad V = \frac{Q_p}{Q_{p0}} \quad \tau = \omega_1 t \quad Y = \frac{S}{h}$$
$$U = \frac{I}{I_0} \quad \omega_1 = \sqrt{\frac{2(k_c - mgA)}{M_1}} \quad \bar{d}(x_1) = \frac{h}{Q_{p0}}\mathrm{d}(q_1)$$
$$M_1 = 2m + M + m_3$$
$$M_2 = M + m_3 \quad M_0 = M + 2m + m_0 + m_3$$
$$\mu_1 = \frac{c_1}{M_1\omega_1} \quad \gamma_1 = \frac{m_3 l}{M_1 h} \quad \beta_1 = \frac{2mAL}{M_1}$$
$$\alpha_1 = \frac{Ak_b L}{\omega_1 M_1} \quad \delta_1 = \frac{Q_{p0}^2}{M_1 C_p \omega_1^2 h^2} \quad \mu_2 = \frac{c_2}{M_2\omega_1}$$
$$\omega_2 = \frac{1}{\omega_1}\sqrt{\frac{k_b}{M_2}} \quad G_2 = \frac{g}{\omega_1^2 L} \quad \alpha_2 = \frac{Ak_b h^2}{2M_2\omega_1^2 L} \quad \gamma_2 = \frac{m_3 l}{M_2 L}$$
$$\delta_2 = \frac{BQ_{p0}}{2C_p M_2 \omega_1^2 L} \quad \delta_m = \frac{M_2 L}{M_0 h} \quad \mu_0 = \frac{c_0}{M_0\omega_1}$$
$$\omega_0 = \frac{1}{\omega_1}\sqrt{\frac{k_0}{M_0}} \quad G_0 = \frac{M_1 g}{M_0\omega_1^2 h} \quad \beta_3 = \frac{KI_0}{M_0\omega_1^2 h}$$
$$\beta_4 = \frac{2mAh}{M_0} \quad \gamma_0 = \frac{m_3 l}{M_0 h} \quad \delta_4 = \frac{BL^2}{4R_p C_p \omega_1 h}$$
$$\mu_3 = \frac{c_3}{\omega_1 m_3 l^2} \quad \omega_3 = \frac{1}{\omega_1}\sqrt{\frac{k_3}{m_3 l^2}} \quad \gamma_3 = \frac{h}{l} \quad \gamma_5 = \frac{g}{\omega_1^2 l}$$
$$\beta_5 = \frac{Kh}{L_0 I_0} \quad \rho = \frac{R_0}{\omega_1 L_0} \quad \Omega = \frac{\omega_n}{\omega_1} \quad E_0 = \frac{e_0}{\omega_1 L_0 I_0}$$
$$\delta_3 = \frac{1}{R_p C_p \omega_1} \quad \varepsilon = \frac{h}{L} \quad (21)$$

To calculate the harvested power, equations (22) and (23) are given as dimensional and dimensionless harvested power, respectively

$$P = R\dot{Q}_p^2 \quad (22)$$

$$P = R_0 V'^2 \quad (23)$$

where $R_0 = R(\omega_1 Q_{p0})^2$.

The average power of the system can be calculated by equation (24)

$$P_{avg} = \frac{1}{T}\int_0^T P(\tau)\mathrm{d}\tau \quad (24)$$

In the next section, numerical simulations will be discussed with and without the usage of the pendulum considering the nonlinear piezoelectric contribution fixed as $\Theta = 1$.

3. Numerical simulations results and discussions

The numerical simulations carried out in this work were performed through the method of Runge–Kutta of fourth and fifth order with a fixed-step $h = 0.001$. The parameters considered for the numerical simulations are in Table 1. These parameters were adjusted to the saturation phenomenon conditions, which are $\omega_2 = 2\omega_1$, and the frequency of the shaker source was

Table 1. Adopted system parameters.

Parameter	Value	Mean
g (m/s^2)	9.81	Gravity acceleration
M (kg)	2.00	Beam mass
m (kg)	0.50	Column mass
m_3 (kg)	Various	Pendulum mass
m_0 (kg)	15.88	Mass of the shaker's base
c_1 (N s/m)	0.001	Column damping
c_2 (N s/m)	0.002	Beam damping
c_3 (N s m/rad)	0.061	Torsional pendulum damping
c_0 (N s/m)	534	Damping of the shaker's base
EI (N m^2)	128	Linear stiffness
k_3 (N m/rad)	0.403	Torsional pendulum stiffness
k_0 (kg/m)	86176	Stiffness of the shaker's base
L (m)	0.52	Beam length
h (m)	0.36	Column length
R_p ($k\Omega$)	100	Piezoelectric resistance
C_p (μF)	1	Piezoelectric capacitance
ω_n (rad/s)	Various	External excitation frequency
θ	0.01	Linear piezoelectric coefficient
Θ	1	Nonlinear piezoelectric coefficient
e_0 (V)	40	Shaker source amplitude
K (N/A)	130	Electromagnetic force of the shaker
L_0 (mH)	2.626	Inductance of the shaker
R_0 (Ω)	0.3	Shaker resistance

set in resonance with the symmetric mode ($\Omega = \omega_2 + \sigma$), where σ is a detuning factor.

All of the parametrical analysis and bifurcation diagrams were obtained using the same initial condition $x_1(0) = 0.01$, which is the displacement of the horizontal direction. Other initial conditions were zero.

A control parameter will be considered in order to configure the system while optimizing its behavior and energy harvesting. This new parameter is defined by equation (25)

$$e = \frac{2m}{m_3} \tag{25}$$

The control parameter e will be varied with an acceptable ratio so that the pendulum mass (m_3) should not exceed the value of the mass of the midspan of the beam (M). This interval is $0.5 \leq e \leq 100$.

The sections below present the results of numerical simulations considering and not considering the passive control and then compare the results showing the efficiency and contribution of the pendulum as a passive controller. All of the numerical simulations were carried out using the parameters in Table 1, except when as described below.

It is highlighted that the parameters are used in the dimensional form for the analysis of the system; however, the numerical analysis and responses of the system are shown in dimensionless form.

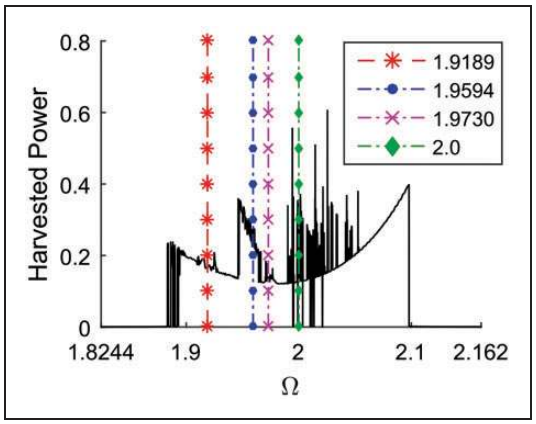

Figure 3. Parametrical analysis of the frequency in relation to the harvested power without a pendulum.

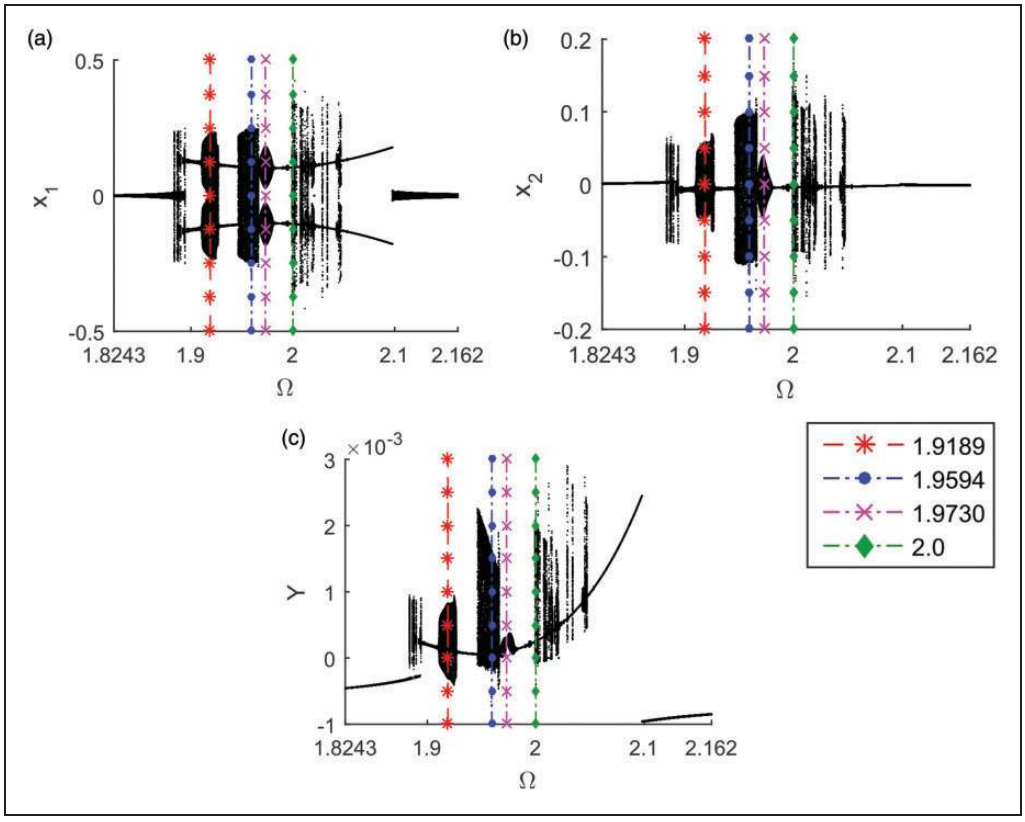

Figure 2. Bifurcation diagram of the system without a pendulum. (a) Horizontal displacement; (b) vertical displacement; (c) base motion.

3.1. Nonlinear dynamical analysis of the platform structure

In the first subsection of numerical simulations, the behavior of the system was analyzed related to the variation of the frequency of the shaker without the coupling of the pendulum. In addition, the harvested power was evaluated. The frequency of the shaker is varied in an interval that satisfies the conditions of the saturation phenomenon, which is near resonance between the shaker and the symmetric direction $\Omega = 2.0$. Thus, the chosen interval is $1.8244 \leq \Omega \leq 2.162$.

Table 2. Cases of non-periodic behaviors.

Case	Frequency	Behavior	Average power
1	1.9189	Quasiperiodic	0.1664
2	1.9594	Quasiperiodic	0.2291
3	1.9730	Quasiperiodic	0.1409
4	2.0	Quasiperiodic	0.2841

First, a bifurcation diagram was built in order to observe the behavior of the system for each value of the frequency of the shaker, illustrated in Figure 2. The analysis of the harvested power related to the frequency is presented in Figure 3.

The bifurcation diagram, shown in Figure 2, shows the interval for which the saturation phenomenon occurs and the system changes its behavior, where the interval is approximately $1.8838 \leq \Omega \leq 2.0973$. Without saturation phenomenon, the system is entirely periodic. When the phenomenon is considered, the system becomes quasiperiodic most of the time.

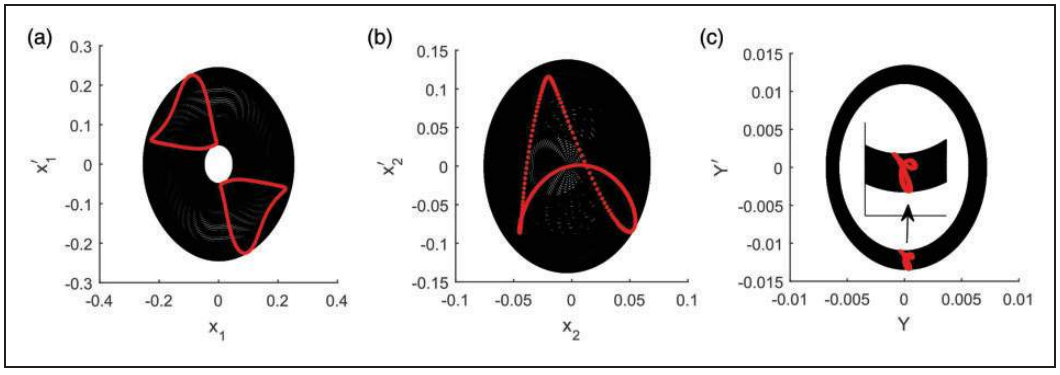

Figure 4. Phase plane (in black) and Poincare maps (in red) of the system without control, $\Omega = 1.9189$. (a) Horizontal motion; (b) vertical motion; (c) base motion.

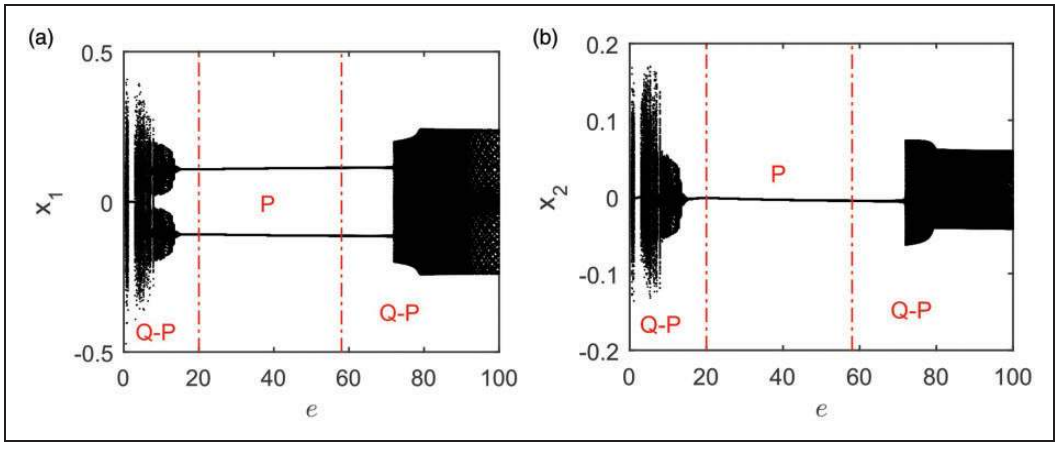

Figure 5. Bifurcation diagrams considering pendulum when $\Omega = 1.9189$, where the red dotted lines represent the interval for e, and P and Q-P represent the periodic and quasi-periodic behaviors, respectively. (a) Horizontal coordinates; (b) vertical coordinates.

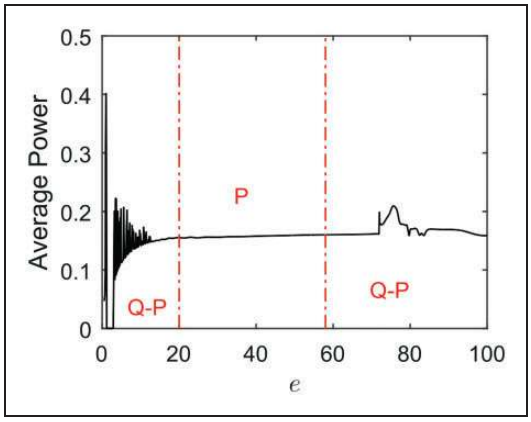

Figure 6. Parametrical analysis of e related to the average harvested power with pendulum, $\Omega = 1.9189$ where the red dotted lines represent the interval for e, and P and Q-P represent the periodic and quasi-periodic behaviors, respectively.

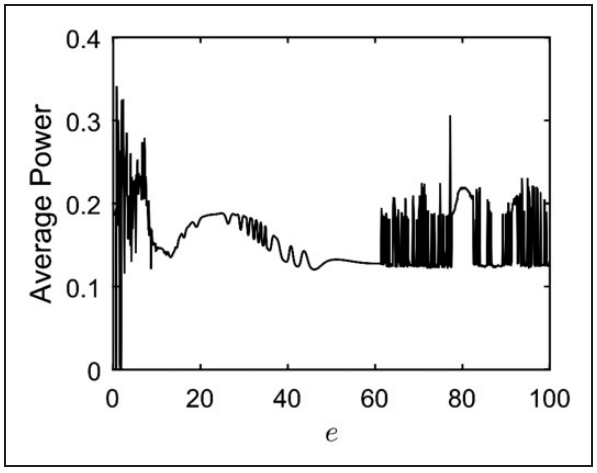

Figure 9. Parametrical analysis of e related to the average harvested power with pendulum, $\Omega = 1.9594$.

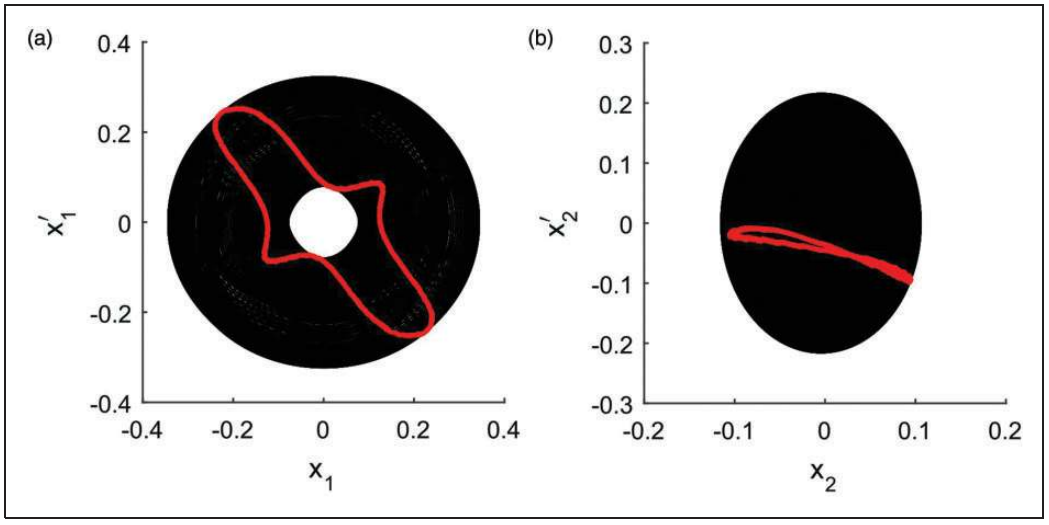

Figure 7. Phase plane (in black) and Poincare maps (in red) of the system without control for $\Omega = 1.9594$. (a) Horizontal motion; (b) vertical motion.

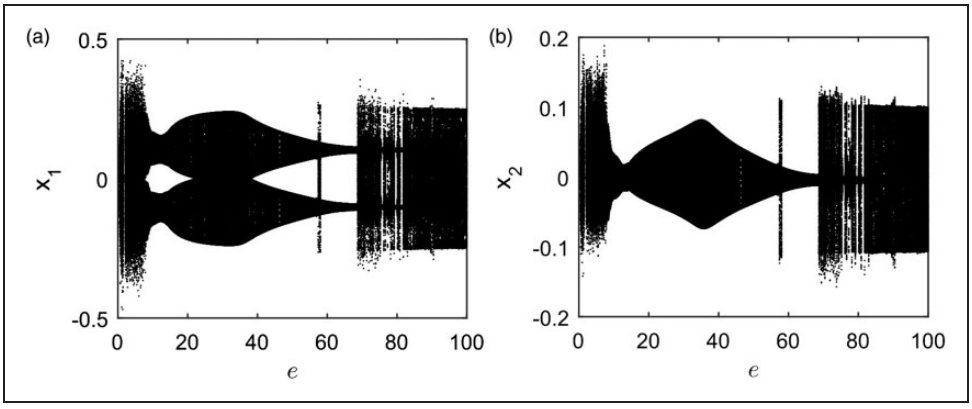

Figure 8. Bifurcation diagrams considering pendulum when $\Omega = 1.9594$. (a) Horizontal coordinates; (b) vertical coordinates.

Figure 2(c) shows the bifurcation diagram for the base motion, which is different from the platform's motion, in the saturation interval, where there is an increase of the amplitude of the base motion. This is due to the increase of the frequency; the velocity of the base increases the change of the axis of oscillation of the base, which does not result in an increase of the amplitude of the base's motion.

In relation to the harvested power, illustrated in Figure 3, when the system presents saturation phenomenon the amount of power greatly increases in comparison to those regions without the phenomenon.

Therefore, we separated four cases of quasiperiodic behavior to apply to the passive controller and seek a periodic solution where we could maintain good energy harvesting. The four cases are shown in Table 2, and are the colored lines in Figures 2 and 3.

In the next section the passive controller is applied in order to study its influence on each case in Table 2.

3.2. Passive control strategy

From this part of this work, the pendulum will be considered to be coupled to the mass M of the mid-span of the beam in order to seek an optimal configuration to find periodic behaviors to maintain energy harvesting.

The following subsections are about the four cases in Table 2, using the passive controller. For the numerical simulations, it is important to study and understand the behavior of the main structure, i.e. the portal frame

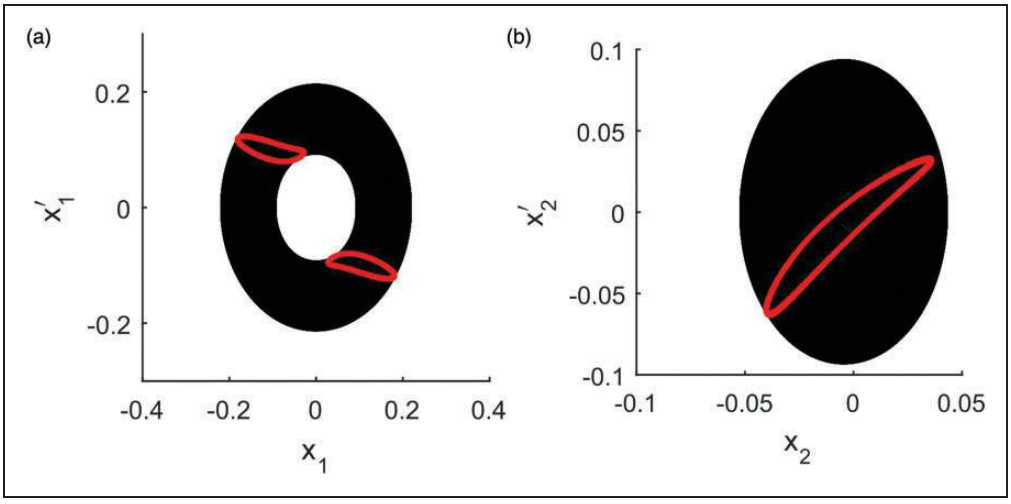

Figure 10. Phase plane (in black) and Poincare maps (in red) of the system without control for $\Omega = 1.9730$. (a) Horizontal motion; (b) vertical motion.

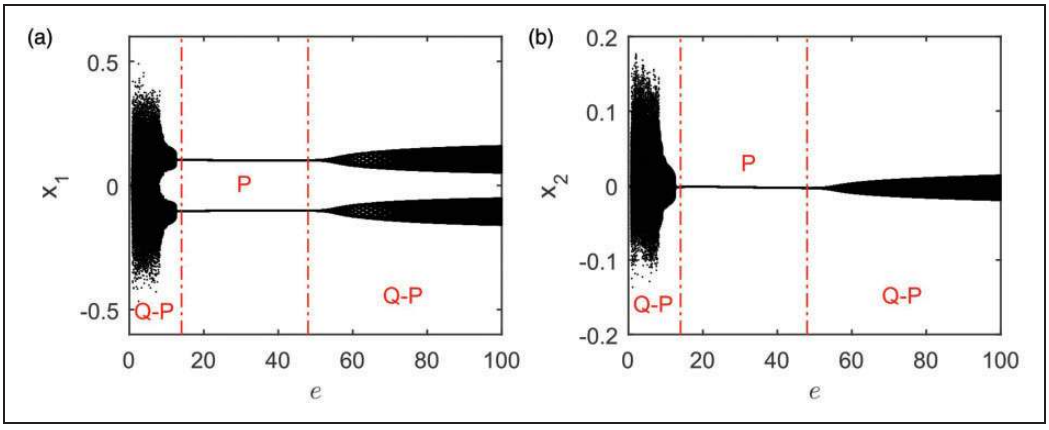

Figure 11. Bifurcation diagrams considering pendulum with $\Omega = 1.9730$ where the red dotted lines represent the interval for e, and P and Q-P represent the periodic and quasi-periodic behaviors, respectively. (a) Horizontal coordinates; (b) vertical coordinates.

platform. Therefore, we will only show the results for x_1 and x_2, although the base and pendulum motions have the same coordinates. Therefore, each case from Table 2 will use the control strategy and study its influence.

3.3. Control of Case 1

In case 1, the frequency is set at $\Omega = 1.9189$. The behavior of the system presents a quasiperiodic orbit as can be seen in the Poincare maps (red line), see Figure 4.

Knowing the quasiperiodic orbit, passive control was considered and then a bifurcation diagram for the two coordinates of the portal frame related to the control parameter e was built, as illustrated in Figure 5, in order to find a periodic orbit. It is possible to see that, in this case, passive control was effective and controlled the quasiperiodic behavior leading to a periodic orbit between the interval $20 \leq e \leq 58$, which is equivalent to $0.0172 \leq m_3 \leq 0.050$ (kg). The periodic behaviors are represented by the area P in Figure 5, between the red dotted lines. The other values of e in the bifurcation diagrams that are quasiperiodic are the limited areas Q-P.

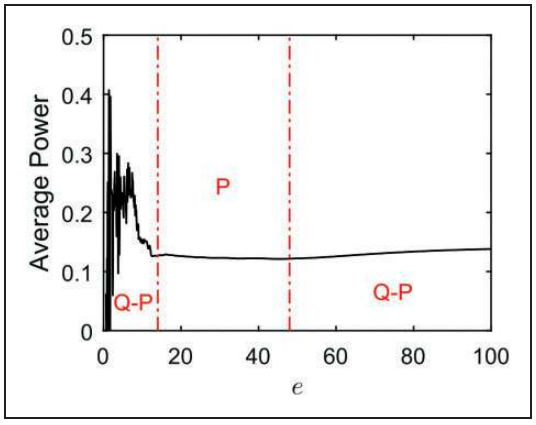

Figure 12. Parametrical analysis of e related to the average harvested power with pendulum, $\Omega = 1.9730$ where the red dotted lines represent the interval for e, and P and Q-P represent the periodic and quasi-periodic behaviors, respectively.

Figure 6 shows the average harvested power with the variation of e. The periodic interval has an average power $0.1556 \leq P_{avg} \leq 0.16$. None of these values are higher than the initial average power in Table 2. However, they are almost of the same value when including the periodic orbit, which is the required behavior for maintaining energy harvesting. Therefore, the passive control was very useful in this case.

3.4. Control of Case 2

In case 2, the frequency is set to $\Omega = 1.9594$ and the system also presents quasiperiodic behavior, as can be seen in the Poincare maps (red line) in Figure 7.

Thus, a bifurcation diagram considering the passive control e is shown in Figure 8. In this case, the passive control was not enough to influence a change of the behavior of the system to keep quasiperiodic behavior, whatever the value of the control parameter. Hence, energy harvesting is not recommended for this frequency.

Figure 9 shows the evaluation of the average harvested power along the e interval.

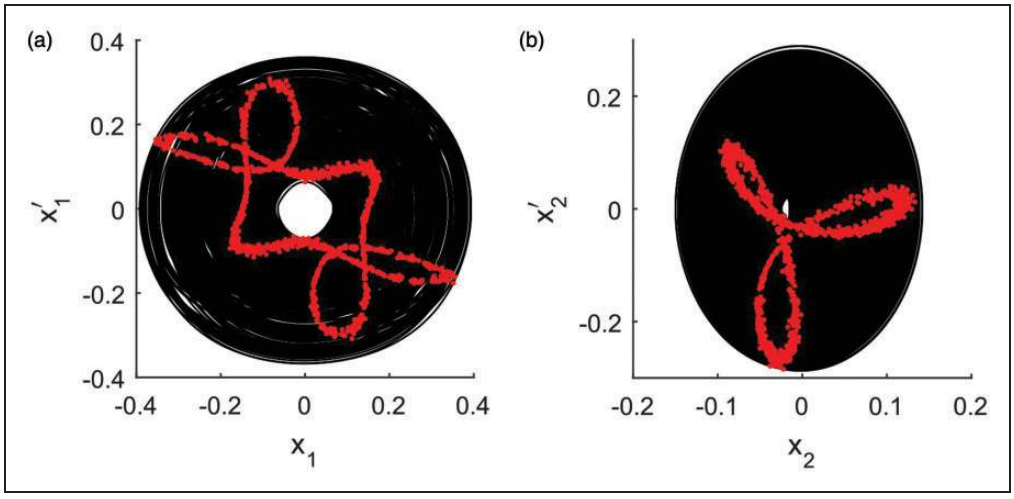

Figure 13. Phase plane (in black) and Poincare maps (in red) of the system without control for $\Omega = 2.0$. (a) Horizontal motion; (b) vertical motion.

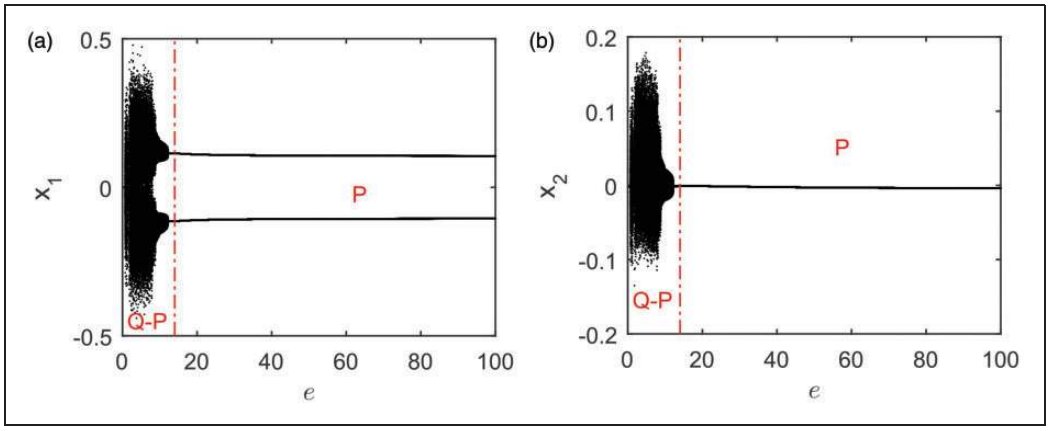

Figure 14. Bifurcation diagrams considering pendulum when $\Omega = 2.0$ where the red dotted lines represent the interval for e, and P and Q-P represent the periodic and quasi-periodic behaviors, respectively. (a) Horizontal coordinates; (b) vertical coordinates.

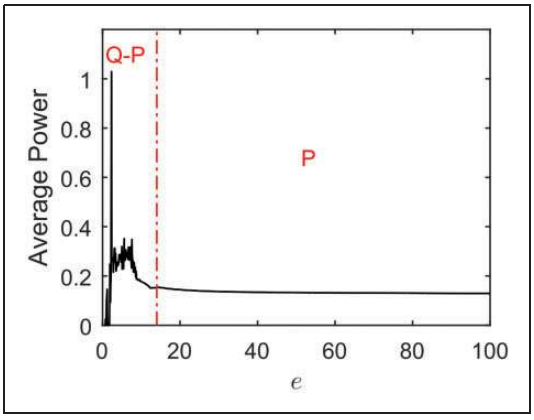

Figure 15. Parametrical analysis of e related to the average harvested power with pendulum, $\Omega = 2.0$ where the red dotted lines represent the interval for e, and P and Q-P represent the periodic and quasi-periodic behaviors, respectively.

Table 3. Summary of the controlled values of the pendulum (periodic behavior).

Case	e	New average power	Original average power
1	$20 \leq e \leq 58$	$0.1556 \leq P_{avg} \leq 0.16$	0.1664
2	Uncontrolled	–	0.2291
3	$14 \leq e \leq 48$	$0.1218 \leq P_{avg} \leq 0.1271$	0.1409
4	$14 \leq e \leq 100$	$0.1296 \leq P_{avg} \leq 0.1526$	0.2841

3.5. Control of Case 3

Case 3 considers the frequency $\Omega = 1.9730$, which is close to case 2. Through the Poincare map (red line) in Figure 10, the system continues to present quasiperiodic behavior.

Therefore, a bifurcation diagram of the system related to the pendulum parameter was constructed in Figure 11. In this case, the pendulum was very effective for the control of quasiperiodic behavior in the interval of approximately $14 \leq e \leq 48$, leading to a periodic orbit. That is equivalent to $0.0208 \leq m_3 \leq 0.0714$ (kg). Hence, in this case is possible to maintain energy harvesting.

Figure 12 shows the average power related to the control parameter. The interval for the amount of harvested power when the system is periodic is $0.1218 \leq P_{avg} \leq 0.1271$. The amount of power in this case is smaller than that of the original, shown in Table 2, which is $P_{avg} = 0.1409$. However, as in case 1, the amount of power is not so much smaller than the original value, therefore, as energy harvesting is possible, and the passive control becomes important.

3.6. Control of Case 4

In case 4, the frequency is set to $\Omega = 2.0$, which is exactly the same condition where saturation phenomenon occurs, i.e. $\Omega = \omega_2 = 2\omega_1 + \sigma$. At this frequency the system also presents quasiperiodic behavior as illustrated in the Poincare map (red line) in Figure 13.

A bifurcation diagram of the system related to the control parameter was built, as illustrated in Figure 14. The system becomes totally controllable in the interval $14 \leq e \leq 100$, i.e. the equivalent to $0.01 \leq m_3 \leq 0.0714$ (kg), which is the interval where the system becomes periodic.

Figure 15 shows the parametrical analysis of the average power related to the control parameter in this case. The average power in the periodic interval is $0.1296 \leq P_{avg} \leq 0.1526$. The values are very much

smaller than those of the original, although the passive controller was very useful.

4. Conclusions

In this work an energy harvesting model of two degrees of freedom with two-to-one internal resonance was presented. The saturation phenomenon was considered, presenting nonperiodic motion as quasiperiodic behavior, which appeared most of the time in the system. Thus, a passive control strategy using a pendulum was proposed and studied in four cases as presented in Table 2, to force the system to behave like a periodic orbit. This kind of behavior is very important and is required to maintain energy harvesting through the piezoelectric material. Therefore, the most important interest in this work is to control the quasiperiodic behaviors for energy harvesting.

The pendulum was shown to be very useful as a controller, as it eliminated the quasiperiodic behavior most of the time, forcing the system to a periodic orbit, depending on the value of the control parameter e.

In cases 1, 3 and 4 the system was controlled by the usage of the pendulum leading their behaviors to a periodic orbit. However, all of them decreased their average harvested power in comparison to the original values. Case 2 was the only case in which it was not possible to control nonperiodic behavior with the pendulum.

Energy harvesting had peaks higher than 0.4 of the amount of power in all four cases. However, the predominant behavior was quasiperiodic, which is not required to harvest energy.

The advantage of using a passive control is that electronic component are not required for the control of the system, in the form of an active or semi-active controller. Therefore, we can tune energy harvesting by choosing a control parameter.

In summary, the conclusions of this work are shown in Table 3.

It is important to note that the results obtained by the use of the passive controller in this work follow the work of Iliuk et al. (2013a, 2013b) and Rocha et al. (2015). The authors have also observed that there is a higher amount of power under chaotic behaviors, and a passive control strategy can be used for energy harvesting when chaos is not desired.

Moreover, the energy harvesting analysis of the system showed that, with irregular motion, the harvested power is higher than when the system has periodic motion. When there is no restriction to the piezoelectric material circuit, it is a valuable option to consider. However, when the electrical components are more sensitive, it is necessary to use strategies that save its physical integrity, therefore reducing the need for complex filters rectifying the energy harvesting output of the system, according to the works of Iliuk et al. (2012, 2013c).

Declaration of Conflicting Interests

The author(s) declared no potential conflicts of interest with respect to the research, authorship, and/or publication of this article.

Funding

The author(s) disclosed receipt of the following financial support for the research, authorship, and/or publication of this article: This work was supported by National Counsel of Technological and Scientific Development (CNPq) (grant numbers 447539/2014-0 and 484729/2013-6), and Coordination for the Improvement of Higher Education Personnel (CAPES).

References

Alevras P, Yurchenko D and Naess A (2014) Stochastic synchronization of rotating parametric pendulums. *Meccanica* 49(8): 1945–1954.

Avanço RH, Navarro HA, Brasil RM, et al. (2015) Statements on nonlinear dynamics behavior of a pendulum, excited by a crank-shaft-slider mechanism. *Meccanica* 1–20.

Balthazar JM, Rocha RT, Brasil RMFL, et al. (2014) Mode saturation, mode coupling and energy harvesting from ambient vibration in a portal frame structure. In: American Society of Mechanica Engineers (ed.) *ASME 2014 international design engineering technical conferences and computers and information in engineering conference*, Buffalo, New York, USA, 17–20 August 2014, pp.V008T11A044–V008T11A044. American Society of Mechanical Engineers.

Crawley EF and Anderson EH (1990) Detailed models of piezoceramic actuation of beams. *Journal of Intelligent Material Systems and Structures* 1(1): 4–25.

Daqaq MF, Masana R, Erturk A, et al. (2014) On the role of nonlinearities in vibratory energy harvesting: A critical review and discussion. *Applied Mechanics Reviews* 66(4): 040801.

DuToit NE and Wardle BL (2007) Experimental verification of models for microfabricated piezoelectric vibration energy harvesters. *AIAA Journal* 45(5): 1126–1137.

Erturk A and Inman DJ (2011) Piezoelectric energy harvesting from aeroelastic vibrations. In: *Piezoelectric energy harvesting*, Wiley, Chichester. DOI:10.1002/9781119991151.

Erturk A, Hoffmann J and Inman DJ (2009) A piezomagnetoelastic structure for broadband vibration energy harvesting. *Applied Physics Letters* 94(25): 254102.

Felix JLP, Balthazar JM and Brasil RM (2005) On saturation control of a non-ideal vibrating portal frame foundation type shear-building. *Journal of Vibration and Control* 11(1): 121–136.

Felix JLP, Silva EL, Balthazar JM, et al. (2014) On nonlinear dynamics and control of a robotic arm with chaos. In: *CSNDD 2014 – International Conference on Structural Nonlinear Dynamics and Diagnosis*, vol. 16, Agadir,

Morocco, 19–21 May, p.05002. MATEC Web of Conferences.

Friswell MI, Bilgen O, Ali SF, et al. (2015) The effect of noise on the response of a vertical cantilever beam energy harvester. *Journal of Applied Mathematics and Mechanics/Zeitschrift für Angewandte Mathematik und Mechanik* 95(5): 433–443.

Golnaraghi MF (1991) Vibration suppression of flexible structures using internal resonance. *Mechanics Research Communications* 18(2–3): 135–143.

Gourdon E, Lamarque CH and Pernot S (2007) Contribution to efficiency of irreversible passive energy pumping with a strong nonlinear attachment. *Nonlinear Dynamics* 50(4): 793–808.

Iliuk I, Balthazar JM, Tusset AM, et al. (2012) Nonlinear dynamics and control strategies: On a energy harvester vibrating system with a linear form to non-ideal motor torque. In: *CSNDD 2012 International Conference on Structural Nonlinear Dynamics and Diagnosis*, Marrakech, Morroco, 30 April–2 May, vol. 1, p.08003. MATEC Web of Conferences, EDP Sciences.

Iliuk I, Balthazar JM, Tusset AM, et al. (2013a) A non-ideal portal frame energy harvester controlled using a pendulum. *The European Physical Journal Special topics* 222(7): 1575–1586.

Iliuk I, Balthazar JM, Tusset AM, et al. (2013b) Application of passive control to energy harvester efficiency using a nonideal portal frame structural support system. *Journal of Intelligent Material Systems and Structures* 25(4): 417–429.

Iliuk I, Balthazar JM, Tusset AM, et al. (2013c) On non-ideal and chaotic energy harvester behavior. *Differential Equations and Dynamical Systems* 21(1): 93–104.

Iliuk I, Brasil RMLRF, Balthazar JM, et al. (2014) Potential application in energy harvesting of intermodal energy exchange in a frame: FEM analysis. *International Journal of Structural Stability and Dynamics*.

Jalili N (2009) *Piezoelectric-Based Vibration Control: From Macro to Micro/Nano Scale Systems*. US: Springer Science & Business Media.

Jiang X, McFarland DM, Bergman LA, et al. (2003) Steady state passive nonlinear energy pumping in coupled oscillators: Theoretical and experimental results. *Nonlinear Dynamics* 33(1): 87–102.

Lenci S and Rega G (2011) Experimental versus theoretical robustness of rotating solutions in a parametrically excited pendulum: A dynamical integrity perspective. *Physica D: Nonlinear Phenomena* 240(9): 814–824.

Lenci S, Brocchini M and Lorenzoni C (2012) Experimental rotations of a pendulum on water waves. *Journal of Computational and Nonlinear Dynamics* 7(1): 011007.

Lenci S, Pavlovskaia E, Rega G, et al. (2008) Rotating solutions and stability of parametric pendulum by perturbation method. *Journal of Sound and Vibration* 310(1): 243–259.

Litak G, Friswell MI and Adhikari S (2016) Regular and chaotic vibration in a piezoelectric energy harvester. *Meccanica* 51(5): 1017–1025.

Litak G, Friswell MI, Kwuimy CAK, et al. (2012) Energy harvesting by two magnetopiezoelastic oscillators with mistuning. *Theoretical and Applied Mechanics Letters* 2(4): 043009. DOI: 10.1063/2.1204309.

Litak G, Wiercigroch M, Horton BW, et al. (2010) Transient chaotic behaviour versus periodic motion of a parametric pendulum by recurrence plots. *Journal of Applied Mathematics and Mechanics/Zeitschrift für Angewandte Mathematik und Mechanik* 90(1): 33–41.

Luongo A and Zulli D (2012) Dynamic analysis of externally excited NES-controlled systems via a mixed multiple scale/harmonic balance algorithm. *Nonlinear Dynamics* 70(3): 2049–2061.

Luongo A and Zulli D (2014) Aeroelastic instability analysis of NES-controlled systems via a mixed multiple scale/harmonic balance method. *Journal of Vibration and Control* 20(13): 1985–1998.

Malatkar P and Nayfeh AH (2007) Steady-state dynamics of a linear structure weakly coupled to an essentially nonlinear oscillator. *Nonlinear Dynamics* 47(1–3): 167–179.

Manevitch LI, Musienko AI and Lamarque CH (2007) New analytical approach to energy pumping problem in strongly nonhomogeneous 2dof systems. *Meccanica* 42(1): 77–83.

Mankala R and Quinn DD (2004) Resonant dynamics and saturation in a coupled system with quadratic nonlinearities. In: *ASME 2004 International Mechanical Engineering Congress and Exposition Design Engineering*, Anaheim, California, USA, 13–19 November 2004, pp. 621–626.

Mook DT, Plaut RH and HaQuang N (1985) The influence of an internal resonance on non-linear structural vibrations under subharmonic resonance conditions. *Journal of Sound and Vibration* 102(4): 473–492.

Musienk AI, Lamarque CH and Manevitch LI (2006) Design of mechanical energy pumping devices. *Journal of Vibration and Control* 12(4): 355–371.

Nayfeh AH (2000) *Nonlinear Interactions*. New York: Wiley.

Nayfeh AH and Mook DT (2008) *Nonlinear Oscillations*. US: John Wiley & Sons, p. 720.

Nayfeh AH, Mook DT and Marshall LR (1973) Nonlinear coupling of pitch and roll modes in ship motions. *Journal of Hydronautics* 7(4): 145–152.

Oueini SS (1999) Techniques for controlling structural vibrations. PhD Thesis, Virginia Tech, US.

Oueini SS, Nayfeh AH and Golnaraghi MF (1997) A theoretical and experimental implementation of a control method based on saturation. *Nonlinear Dynamics* 13(2): 189–202.

Pai PF and Schulz MJ (2000) A refined nonlinear vibration absorber. *International Journal of Mechanical Sciences* 42(3): 537–560.

Pai PF, Wen B, Naser AS, et al. (1998) Structural vibration control using PZT patches and non-linear phenomena. *Journal of Sound and Vibration* 215(2): 273–296.

Preumont A (2006) *Mechatronics: Dynamics of Electromechanical and Piezoelectric Systems*. Vol. 136, Netherlands: Springer Science & Business Media.

Priya S and Inman DJ (eds) (2009) *Energy Harvesting Technologies*. Vol. 21, New York: Springer.

Quinn DD (2007) Resonant dynamics in strongly nonlinear systems. *Nonlinear Dynamics* 49(3): 361–373.

Rocha RT, Balthazar JM, Tusset AM, et al. (2015) Using saturation phenomenon to improve energy harvesting in a portal frame platform with passive control by a pendulum. *Dynamical Systems: Theoretical and Experimental Analysis* Switzerland: Springer International Publishing, pp. 319–329.

Rocha RT, Balthazar JM, Tusset AM, et al. (2016) Comments on energy harvesting on a 2:1 internal resonance portal frame support structure, using a nonlinear-energy sink as a passive controller. *International Review of Mechanical Engineering* 10(3): 147–156.

Shoeybi M and Ghorashi M (2005) Control of a nonlinear system using the saturation phenomenon. *Nonlinear Dynamics* 42(2): 113–136.

Stanton SC, McGehee CC and Mann BP (2010) Nonlinear dynamics for broadband energy harvesting: Investigation of a bistable piezoelectric inertial generator. *Physica D: Nonlinear Phenomena* 239(10): 640–653.

Stephen NG (2006) On energy harvesting from ambient vibration. *Journal of Sound and Vibration* 293(1): 409–425.

Syta A, Bowen CR, Kim HA, et al. (2015) Experimental analysis of the dynamical response of energy harvesting devices based on bistable laminated plates. *Meccanica* 50(8): 1961–1970.

Triplett A and Quinn DD (2009) The effect of non-linear piezoelectric coupling on vibration-based energy harvesting. *Journal of Intelligent Material Systems and Structures* 20(16): 1959–1967.

Tusset AM, Piccirillo V, Bueno AM, et al. (2016) Chaos control and sensitivity analysis of a double pendulum arm excited by an RLC circuit based nonlinear shaker. *Journal of Vibration and Control* 22(17): 3621–3637.

Twiefel J, Richter B, Sattel T, et al. (2008) Power output estimation and experimental validation for piezoelectric energy harvesting systems. *Journal of Electroceramics* 20(3–4): 203–208.

Vakakis AF (2008) *Nonlinear Targeted Energy Transfer in Mechanical and Structural Systems*. Vol. 156, Netherlands: Springer Science & Business Media.

Wang R and Jing Z (2004) Chaos control of chaotic pendulum system. *Chaos, Solitons & Fractals* 21(1): 201–207.

Warminski J, Cartmell MP, Mitura A, et al. (2013) Active vibration control of a nonlinear beam with self-and external excitations. *Shock and Vibration* 20(6): 1033–1047.

Xu X, Pavlovskaia E, Wiercigroch M, et al. (2007) Dynamic interactions between parametric pendulum and electrodynamical shaker. *Journal of Applied Mathematics and Mechanics/Zeitschrift für Angewandte Mathematik und Mechanik* 87(2): 172–186.

Xu X, Wiercigroch M and Cartmell MP (2005) Rotating orbits of a parametrically-excited pendulum. *Chaos, Solitons & Fractals* 23(5): 1537–1548.

Yokoi Y and Hikihara T (2011) Tolerance of start-up control of rotation in parametric pendulum by delayed feedback. *Physics Letters A* 375(17): 1779–1783.

Zulli D and Luongo A (2015) Nonlinear energy sink to control vibrations of an internally nonresonant elastic string. *Meccanica* 50(3): 781–794.